A Physics-Informed Neural Network Approach to the Richards Equation and Soil-Process Investigation

Ivan Maltsev
ISP RAS
Moscow, Russia
e-mail: i.maltsev@ispras.ru

Sergei Strijhak
ISP RAS
Moscow, Russia
e-mail: s.strijhak@ispras.ru

Anna Varlamova
ISP RAS
Moscow, Russia
e-mail: a.varlamova@ispras.ru

Andrei Kulinskii
ISP RAS
Moscow, Russia
e-mail: a.kulinsky@ispras.ru

***Abstract*—This paper presents a physics-informed neural network (PINN) approach for solving the Richards equation, which governs transient moisture transport in variably saturated soils. The model is trained on synthetic datasets generated using the *porousMultiphaseFoam* library based on OpenFOAM. The study investigates the ability of PINNs to accurately reproduce one- and two-dimensional infiltration dynamics and predict moisture content profiles over time.**

***Keywords*—Soil, Richards equation, domain, numerical, solution, saturation, hydraulic, physics-informed neural networks, prediction, MSE.**

I. Introduction

The Richards equation describes moisture transport in unsaturated soils, linking hydraulic head and saturation through nonlinear soil properties. Numerical solvers such as APSIM, ParFlow and *porousMultiphaseFoam* (OpenFOAM) are widely used to solve it.

Physics-informed neural networks (PINNs) embed these governing equations in their loss functions, enabling physically consistent learning. PINNs have shown success in fluid and porous media modeling [1] and in soil-specific tasks such as approximating the soil water retention curve [2-6], but their hydrological applications remain limited.

This paper explores the use of PINNs for 1D and 2D infiltration problems based on the Richards equation, contributing to the development of digital twin models in soil hydrology.

II. Mathematical Model

A. Darcy and Richards Equations

Darcy's filtration law for liquids and gases, formulated in 1856 in differential form, applies only to saturated media. In vector notation, it reads:

$$q \;=\; -\frac{K}{\mu}\,\nabla\big(\rho g z + P\big), \tag{1}$$

where $\mathbf{q}$ is the vector of the filtration velocity, K – the intrinsic permeability, μ – the dynamic viscosity, P – the fluid pressure, ρ – the density, g – the gravitational acceleration and z – the vertical coordinate. Introducing the hydraulic head $h = \dfrac{P}{\rho g} + z$ yields the familiar form

$$q \;=\; -K_s\,\nabla h, \tag{2}$$

with $K_s = \dfrac{\rho g}{\mu}\,K$ – the saturated hydraulic conductivity.

In 1931, Lorenzo Richards generalized Darcy's idea Eq. (2) and obtained the filtration law in its full form:

$$\begin{aligned}\frac{\partial\theta}{\partial t} \;+\; \frac{\theta S_s}{\varepsilon}\,\frac{\partial h}{\partial t} \;-\; \nabla\Big(\frac{K\,\rho\|g\|_2}{\mu}\,k_{r,h}\,\nabla h\Big) \\ +\; \nabla\Big(\frac{K\,\rho g}{\mu}\,k_{r,h}\Big) \;=\; Q_{\text{source}}.\end{aligned} \tag{3}$$

where θ is the volumetric water content, the term $\dfrac{\theta S_s}{\varepsilon}\,\dfrac{\partial h}{\partial t}$ represents the contribution of aquifer storage, $k_{r,h}$ is the relative permeability, and Q_{source} is a source term.

Rewriting the governing equation in terms of hydraulic head gives

$$C(h)\,\frac{\partial h}{\partial t} - \nabla\left(\frac{K\,k_{r,h}\,\rho}{\mu}\left(\|g\|_2\,\nabla h - g\right)\right) = 0, \tag{4}$$

Here, $C(h)$ is the capillary capacity and $k_{r,h}$ is the relative permeability. Both are expressed through the soil water retention curve.

$$\theta(h) = \begin{cases} \dfrac{\theta_s - \theta_r}{\big(1 + (\alpha|h|)^n\big)^m} + \theta_r, & h < 0, \\ \theta_s, & h \geq 0, \end{cases} \tag{5}$$

and the effective saturation

$$\theta_e = \frac{\theta(h) - \theta_r}{\theta_s - \theta_r}. \tag{6}$$

With these definitions, the capillary capacity becomes

$$C(h) = \frac{\partial\theta}{\partial t} = \frac{\alpha m(\theta_s - \theta_r)}{1 - m}\left(\theta_e^{\frac{1}{m}}\right)\left(1 - \theta_e^{\frac{1}{m}}\right)^m, \tag{7}$$

and the relative permeability is

$$k_{r,h} = \sqrt{\theta_e}\left[1 - \left(1 - \theta_e^{1/m}\right)^m\right]^2. \tag{8}$$

https://doi.org/10.51408/csit2025_65

In these expressions, θ_s, θ_r are the saturated and residual water contents, respectively; α, m are parameters of the van Genuchten model, and θ_e is the effective saturation.

III. Capabilities of the *porousMultiphaseFoam* Library

The *porousMultiphaseFoam* library, implemented in OpenFOAM-v2306, provides a suite of solvers for saturated and variably saturated flow, including coupled water solute transport. It supports GIS-based preprocessing, scalar transport for multiple species, and custom porous-media boundary conditions.

All solvers have been validated against the benchmark cases [7], [8], which confirms high accuracy. The main solver, *groundwaterFoam*, uses implicit time stepping with the Picard iteration. This makes the library suitable for generating synthetic datasets for training physics-informed neural networks.

IV. Problem Setup

To solve the Richards equation, four contrasting soil types were selected. The first three are from Russia: (1) a gray forest medium loam from the Vladimir region with compacted horizons and fissure-like pores; (2) a sod-podzolic loam from the Moscow region with small biogenic channels and fine cracking [9]; and (3) a Chernozem from the Central Altai with granular structure and low bulk density [10]. The fourth is a reference sandy loam from New Mexico, USA, with high porosity and saturated hydraulic conductivity [11].

A. One-Dimensional Case

In the 1D scenario, the PINN takes (z, t) as input and returns $h(z, t)$. We model sandy loam from New Mexico using boundary and initial conditions:

$$h(0,t) = -0.75 \text{ m}, \qquad h(-0.6,t) = -10 \text{ m},$$
$$h(z,0) = -10 \text{ m}, \qquad z \in [0, -0.6].$$

The Richards equation is defined as:

$$\text{pde}(h) = -\frac{1}{95\,000}\Big[\frac{\partial h}{\partial t} + \frac{K\rho}{95\,000\,\mu\,C(h)}\Big(\frac{\partial k(h)}{\partial z}(|g|\partial_z h - g) + k(h)|g|\,\partial_z^2 h\Big)\Big]. \tag{9}$$

The time domain [0, 95,000 s] is scaled to [0,1]. Soil properties: $K = 9.4 \times 10^{-12}\,\text{m}^2$, $\theta_s = 0.368$, $\theta_r = 0.102$, $\alpha = 3.35\,\text{m}^{-1}$, $m = 0.5$, $\mu = 10^{-3}\,\text{Pa s}$, $\rho = 10^3\,\text{kg m}^{-3}$.

B. Two-Dimensional Case

In the 2D case, the input becomes (x, z, t). The governing PDE extends to spatial derivatives in x:

$$\text{pde}(h) = -\frac{1}{95\,000\,C(h)}\Big\{C(h)\,\partial_t h - \nabla\cdot\left(\frac{K(h)k(h)}{\mu}\,[\rho|g|(\partial_x h + \partial_z h) - \rho g]\right)\Big\} \tag{10}$$

An isotropic medium with constant permeability (from K_s) is assumed. The parameters for all four soils are listed in Table I, including h_{top} in $z \in (0.2, 0.3)$, h_{bot} in $z = -0.6$, and $h_0 = h(z, 0)$.

TABLE I: Hydro-physical parameters and boundary/initial conditions for four soil types

	Sandy loam	Cherno zem	Sod-podzolic	Grey forest
K_s (m s^{-1})	9.22×10^{-5}	1.02×10^{-5}	3.47×10^{-6}	9.49×10^{-6}
θ_r	0.102	0.0354	0.034	0.075
θ_s	0.368	0.459	0.45	0.47
α (m^{-1})	3.35	0.54	1.6	0.7
n	2.0	1.5362	1.37	1.6
h_{top} (m)	-0.75	-0.5	-0.5	-0.5
h_{bot} (m)	-10	-2.8	-3.6	-3.2
h_0 (m)	-10	-2.8	-3.6	-3.2

V. PINN Architecture

Using the Python scientific machine-learning library *DeepXDE*, a fully connected neural network was built to solve the Richards equation in one dimension [2]. The network contains three hidden layers with 20 neurons each (Figure 1).

For the two-dimensional case, the PINN takes the vector (x, z, t) as input and outputs the hydraulic head h. The fully connected network consists of five layers with 50 neurons each (Figure 2). The other parameters are in Table II.

TABLE II: Model parameters

Case	Layers	Neurons	Activation	Optimiser	Learning rate
1D	3	20	Tanh	Adam	10^{-3}
2D	5	50	ReLU	Adam	10^{-3}, 10^{-4}

VI. Results

A. One-Dimensional case

After 100,000 training epochs, the network produces the hydraulic head profiles shown in Fig. 3(a). The reference solution obtained with *porousMultiphaseFoam* is shown in Fig. 3(b).

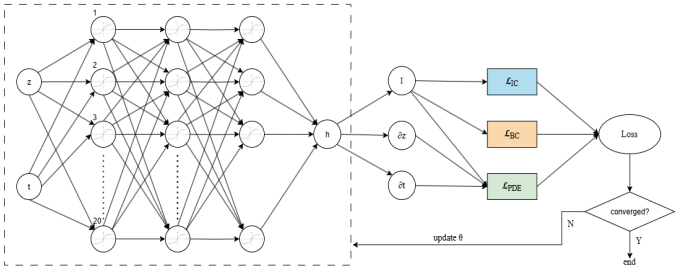

Fig. 1: PINN architecture for the 1D case

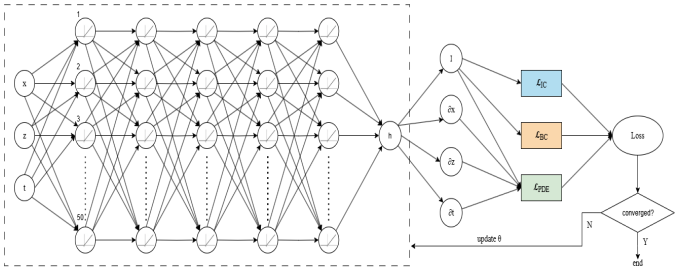

Fig. 2: PINN architecture for the 2D case

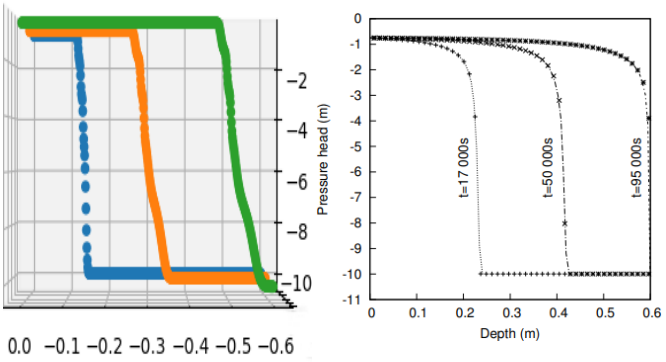

(a) PINN solution for the 1D problem at three time instants

(b) Reference solution obtained with *porousMultiphaseFoam*

Fig. 3: Comparison of (a) PINN and (b) reference solutions for the 1D case

Incorporating a small subset of numerical data from *porousMultiphaseFoam* in the training process reduces the mean squared error (MSE) to 9.6×10^{-3} after 16,000 epochs. Here, a calculation was performed for 1,000 seconds. The results of the comparison between the calculated solution and the PINN-based approximation for the function h are presented in Figure 4. Judging by the results obtained, PINN has indeed learned to approximate the solution obtained by the numerical method very closely; however, it is notable that the greatest discrepancies in the results were reached when approximating the values at the lower bound. The behavior of the MSE metric during the training process is shown in Figure 5.

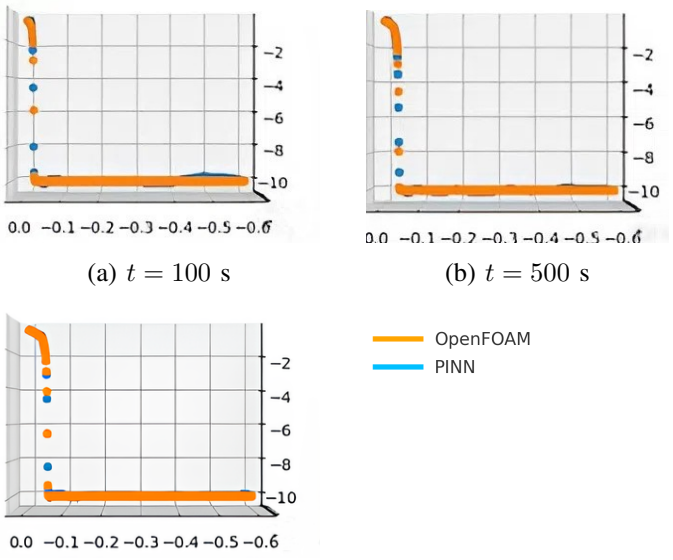

(a) $t = 100$ s

(b) $t = 500$ s

(c) $t = 900$ s

Fig. 4: PINN predictions of hydraulic head in the 1D setting at different time steps

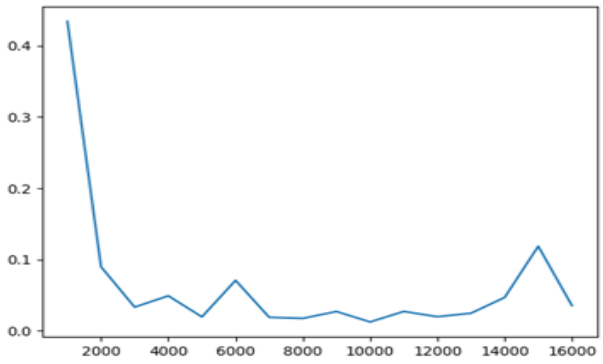

Fig. 5: MSE for the 1D case

B. Two-Dimensional case

In the 2D isotropic formulation, a deeper network trained with stepwise learning rate decay reproduces the head dynamics over a wide permeability range. Training was carried out for 40,000 epochs with an initial learning rate of 10^{-3}; the rate was reduced by one order after the first 20,000 epochs. The loss history plots are presented in Fig. 6.

As shown in Fig. 7, the gray forest soil develops a smooth saturation gradient - the wetting front is diffuse and gradually fades with depth, matching its high matrix porosity and water holding capacity. In sod-podzolic soil, water infiltrates much more efficiently because of its lower bulk density, producing a steeper but still continuous front. The Chernozem displays a sharply defined wetting boundary: water is quickly absorbed from above and then held back by the fine-pored organo-mineral matrix, so the front stalls and remains compact. Sandy loam soil in New Mexico is the most rapidly and deeply moistened of all samples: the coarse pore skeleton conducts water rapidly downward, giving the profile a sudden jump in water content and leaving little moisture stored in the matrix.

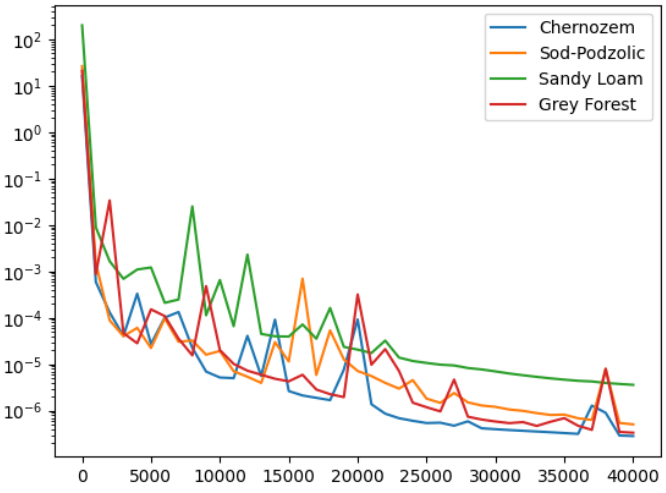

Fig. 6: Loss history plots for considered soil types

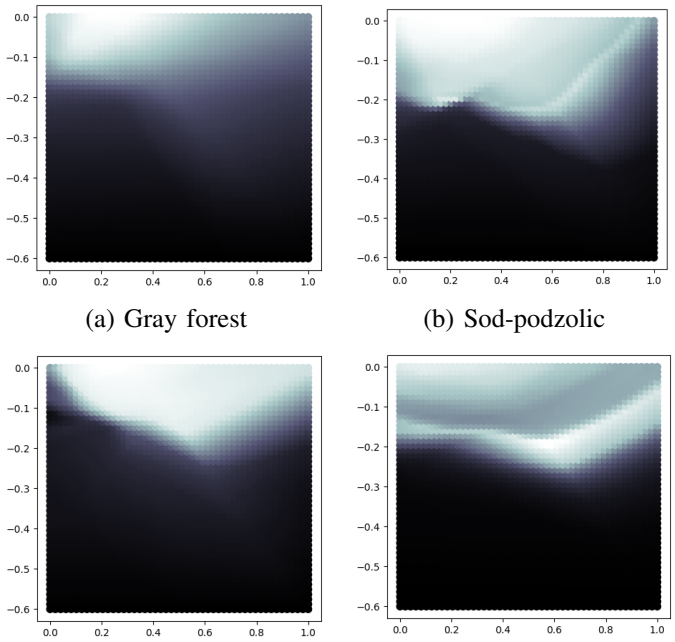

(a) Gray forest (b) Sod-podzolic

(c) Chernozem (d) Sandy loam

Fig. 7: Saturation fronts at $t = 28\,500$ s in the 2D isotropic setting for four soil types

VII. Discussion

PINNs show promise, but several gaps remain. (1) We used only a fully connected architecture; operator-learning models such as DeepONet [12] and FNO [13] merit evaluation. (2) Hyperparameters (learning rate, depth/width, optimizer) were not tuned; automated HPO (e.g., *Optuna*) should be applied. (3) Realistic digital twins require a 3D Richards formulation. (4) Robust benchmarking needs quantitative comparisons against data-driven and physics-informed baselines. Addressing these items will improve robustness and practical utility in geoscience and agro-environmental applications.

VIII. Conclusion

Several neural-network approaches to solving the Richards equation have been explored, and the DeepXDE library has been tested to train PINNs [2]. The analysis shows that the highest accuracy is achieved when synthetic data are included in the training process.

To train PINN, the NVIDIA Tesla T4 GPU was used. It is a powerful graphics accelerator with 16 GB GDDR6 video memory. The training process for each case took about 2.5 minutes.

Comparing the PINN 1D predictions with *porousMultiphaseFoam* results reveals that the baseline PINN correctly reconstructs the shape of the wetting front, while incorporating synthetic data yields quantitative agreement with the classical solution. These findings highlight the potential of PINNs for studying multidimensional soil processes and parameter-uncertain problems, confirming their suitability for use in digital twins of agro-systems to provide rapid forecasts of soil-water regimes. Having a number of soil parameters, it is possible to assume the nature of the moisture seepage process. For example, the K_s parameter is a key parameter for the seepage rate, and α is a suction parameter that determines the water retention curve (the lower α, the slower drying). The results of the PINN simulation for the 2D case show results consistent with the initial assumptions:

1) In the Gray forest soil, moisture is evenly distributed, penetrates deeply, but slowly;
2) Sod-podzolic soil is similar in properties to gray forest soil, but has better suction properties;
3) In Chernozem, moisture spreads deeper and lasts longer.;
4) In Sandy loam, water moves quickly, but does not linger.

Future work may focus on evaluating alternative network architectures – such as DeepONet and Fourier Neural Operators – and on integrating PINNs with various mathematical models to further investigate soil processes.

Acknowledgment

The work was carried out with the financial support of the Ministry of Science and Higher Education of the Russian Federation (Agreement No. 075-15-2024-545 dated April 24, 2024).

References

[1] M. Raissi, P. Perdikaris, and G. E. Karniadakis, "Physics-informed neural networks: A deep-learning framework for solving forward and inverse problems involving nonlinear partial differential equations," *J. Comput. Phys.*, vol. 378, pp. 686–707, 2019.

[2] L. Lu, X. Meng, Z. Mao, and G. E. Karniadakis, "DeepXDE: A deep-learning library for solving differential equations," *arXiv preprint* arXiv:1907.04502, 2019.

[3] I. Depina *et al.*, "Application of physics-informed neural networks to inverse problems in unsaturated groundwater flow," *Georisk*, vol. 15, no. 4, pp. 301–313, 2021.

[4] T. Bandai and T. A. Ghezzehei, "Forward and inverse modelling of water flow in unsaturated soils with discontinuous hydraulic conductivities using physics-informed neural networks with domain decomposition," *Hydrol. Earth Syst. Sci.*, vol. 26, pp. 4469–4495, 2022.

[5] Y. Yang and G. Mei, "A deep-learning-based approach for a numerical investigation of soil–water vertical infiltration with physics-informed neural networks," *Mathematics*, vol. 10, no. 16, 2022.

[6] Y. Chen, Y. Xu, L. Wang, and T. Li, "Modelling water flow in unsaturated soils through physics-informed neural networks," *Comput. Geotech.*, vol. 161, 105546, 2023.

[7] P. Horgue *et al.*, "An open-source toolbox for multiphase flow in porous media," *Comput. Phys. Commun.*, vol. 187, pp. 217–226, 2015.

[8] P. Horgue *et al.*, "porousMultiphaseFoam v2107: An open-source tool for modelling saturated/unsaturated water flows and solute transfers at watershed scale," *Comput. Phys. Commun.*, vol. 273, 108278, 2022.

[9] S. S. Panina, "Water movement in soil under low- and zero-head infiltration," Ph.D. thesis, Lomonosov Moscow State Univ., 2015.

[10] S. V. Baboshkina *et al.*, "Moisture movement in chernozems of the Uimon depression, Central Altai," *Adv. Curr. Nat. Sci.*, no. 12, pp. 133–138, 2016.

[11] P. Horgue *et al.*, "Extension of porousMultiphaseFoam for groundwater flow (Richards' equation)," Tech. Rep., IMFT, 2015.

[12] L. Lu *et al.*, "Learning nonlinear operators via DeepONet based on the universal approximation theorem of operators," *Nature Machine Intelligence*, vol. 3, no. 3, pp. 218–229, 2021.

[13] Z. Li, N. Kovachki, K. Azizzadenesheli, B. Liu, K. Bhattacharya, A. M. Stuart, and A. Anandkumar, "Fourier neural operator for parametric partial differential equations," in *Proc. Int. Conf. Learning Representations (ICLR)*, 2021, arXiv:2010.08895.